J. Iran. Chem. Soc., Vol. 5, No. 3, September 2008, pp. 436-444.

JOURNAL OF THE
Iranian
Chemical Society

Antipyrilquinoneimine Dye Formation by Coupling Aniline Derivatives with 4-Aminoantipyrine in the Presence of Ruthenium Nanoparticles

J. Kasthuri[a], J. Santhanalakshmi[b,]* and N. Rajendiran[c]
[a]*Department of Chemistry, S.R.M. University, Faculty of Engineering and Technology, Chennai-603 203*
[b]*Department of Physical Chemistry, University of Madras, Guindy Campus, Chennai-600 025, India*
[c]*Department of Polymer Science, University of Madras, Guindy Campus, Chennai-600 025, India*

(Received 3 September 2007, Accepted 2 November 2007)

The coupling of 4-aminoantipyrine (4-AAP) with aniline derivatives catalyzed by ruthenium nanoparticles (Rnp) has been studied by UV-Vis spectroscopy in aqueous medium. The rate constant for antipyrilquinoneimine dye formation depends on the nature of the aniline substituent and the pH, ionic strength and temperature of the reaction medium. The maximum rate constant of the dye formation reaction is observed at pH 3.6. Aniline derivatives with electron donating substituents show higher rate constant values than those with electron withdrawing substituents, with increasing rate constant values in the order: N,N-dimethyl aniline > *o*-toluidine > *o*-chloroaniline > *m*-chloroaniline. With pseudo first order kinetics, the total order is 1.0 + 1.0 + 1.0 = 3.0, which includes the orders with respect to amine, 4-AAP and Rnp. Studies on these effects help to complete the kinetic analysis as well as propose the reaction pathway. Furthermore, TEM measurement confirms that the nanoscalar size of the Rnp is 7 nm.

Keywords: Antipyrilquinoneimine dyes, Coupling reaction, Anilines, Reaction kinetics, Ruthenium nanoparticles

INTRODUCTION

Aromatic amines are of growing significance in environmental chemistry due to their hazardous wastes and potential carcinogenic properties [1,2]. Many other industrial applications, such as the manufacturing of dyes, cosmetics, medicines and rubber, release wastes into streams with concentrations as high as 10 g l^{-1} [3,4]. Because of their threat to the environment, different methods have been developed to provide a rapid and sensitive means to detect these compounds [5-8]. In this context, oxidative coupling reactions of amines in the presence of chromogenic electron donor species provide a way to have a simple quantitative photometric assay to determine the formation of the reaction product. So that adequate processes can be developed and implemented, there is a fundamental need to understand the kinetics of the system, as this is essential for process design and optimization of the operation. In earlier studies, the reaction between aniline and phenol with 4-AAP in the presence of H_2O_2 catalyzed by tetrasulfophthalocyanine was found to produce an intense pink and red-colored water-soluble dye product that is precisely and easily detected and estimated using UV-Vis spectroscopy [9,10].

In continuation of our earlier work, we now report a dye formation reaction between 4-AAP and aniline derivatives in the presence of ruthenium nanoparticles (Rnp) as a catalyst without the addition of H_2O_2 as an oxidant. The dye formation reaction does not proceed without a catalyst [11]. However, the addition of Rnp into the reaction mixture containing aniline derivatives with 4-AAP causes the formation of

---

*Corresponding author. E-mail: drjslakshmi06@yahoo.co.in characteristic colors of the respective antipyrilquinoneimine dye. The kinetics of the dye formation can be monitored by UV-Vis spectroscopy at various time intervals at the characteristic λ_{max} of the corresponding dye. The catalytic activity of Rnp in aqueous medium is of great interest due to its greater stability, higher number of active sites on the surfaces of smaller particles, leading to higher rate constants for many reactions [12-15].

The coupling reaction of anilines with 4-AAP involves the formation of a [C_B = N-] bond, where C_B is the benzene ring carbon of the aniline derivative and N belongs to the amino group of the 4-AAP molecule. This can be confirmed by the characteristic peak at 1635 cm^{-1} for N,N-dimethyl aniline (DMA) system in its FT-IR spectra. In this study, the maximum rate constant of the reaction is optimized by investigating the effects of various compositions of aniline derivatives, 4-AAP, Rnp, ionic strength, pH and temperature of the reaction medium. We further calculate the rate constants and activation energies from the resultant slope values. We clarify the interactions of aniline derivatives with 4-AAP using these kinetic parameters, and analyze the role of Rnp in the reaction pathway.

EXPERIMENTAL

General

The chemicals were purchased from Aldrich chemical company or Loba-Chemie India Ltd. and were used without further purification. All solutions were prepared using double-distilled water. UV-Vis spectroscopic measurements were performed on a Shimadzu UV-1601 double beam spectrophotometer. The optical length of the quartz cuvette was 1 cm. FT-IR spectra of the dye formed between DMA and 4-AAP in the presence of Rnp were recorded using KBr pellets at 25 ºC from 500 cm^{-1} to 4000 cm^{-1} on a Perkin-Elmer instrument. An Elico-India digital pH meter was used to measure pH. Cyclic voltammograms of the aqueous solutions of the reactants containing Rnp were obtained using EG&G PAR 283 potentiostat/galvanostat. The TEM photograph was taken on a JEOL model 1200 EX instrument operated at an accelerating voltage of 120 kV.

Synthesis of Ruthenium Nanoparticles in Aqueous Medium

The basic polyol method was followed to obtain Rnp with the capping agent as poly(N-vinyl-2-pyrrolidone) (PVP) [16]. Rnp was prepared in a three-necked round bottom flask, fitted with stirrer and a condenser, following the reported procedure with slight modifications [17]. We dissolved 11 mg of uthenium trichloride trihydrate ($RuCl_3.3H_2O$) in 5 ml of ethylene glycol (EG). To this, 250 mg of PVP dissolved in 20 ml of EG was added. The resulting reaction mixture was heated up to 150 ºC with constant stirring and the resultant dark honey colored solution confirmed the formation of ruthenium nanoparticles. The stability of the colloidal dispersion was ascertained by maintaining the solution at -5 ºC in a cryostat for 1 h.

Kinetic Measurements

All reactions were carried out with fresh solutions only. The initiation of the reaction was considered as the time of the addition of Rnp into the reaction mixture containing aniline derivatives and 4-AAP. As the reaction proceeds, the absorbance value increases with time. The kinetic plots comprising logX *vs*. time, where X = $[(OD_\infty)/(OD_\infty - OD_t)]$ and OD_t and OD_∞ refers to absorbance at time ‘t’ and at completion of reaction, respectively. The kinetic plots were used to determine the rate constant values by maintaining 4-AAP concentration nearly 10 times greater than the amine concentration in accordance with pseudo first order conditions. The exact concentration of the substrates and the catalyst to be employed in the studies on other external effects, including ionic strength, pH and temperature, were deduced from these results. For such purposes, the concentration of Rnp and aniline derivatives were optimized.

RESULTS AND DISCUSSION

Effect of Substituent on Aniline Derivatives

The UV-Vis stacked spectra of the dye formation reaction between 4-AAP and N,N-dimethyl aniline in the presence of the Rnp catalyst at different time intervals are shown in Fig. 1. Note the spectral changes that occur upon the addition of Rnp to the reaction mixture. In this study, we examined the effect of four different aniline derivatives, including N,N-dimethyl aniline (DMA), *o*- toluidine, *o*-chloro aniline (*o*-Cl-Ani), and *m*-chloro aniline (*m*-Cl-Ani), on the reaction with 4-AAP using Rnp as a catalyst. The shift in the λ_{max} position of the

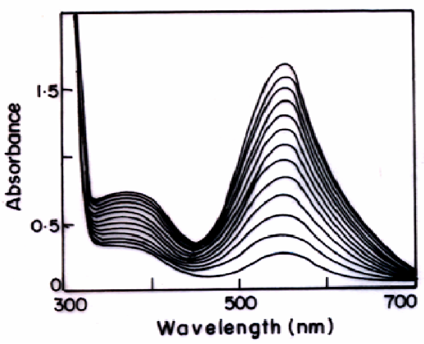

Fig. 1. UV-Vis stacked spectra at different time intervals during the reaction between DMA and 4-AAP with the Rnp catalyst in water at 25 ºC. [DMA] = 1.79 × 10^{-3} M, [4-AAP] = 1.50 × 10^{-2} M, [Rnp] = 2.44 × 10^{-3} M.

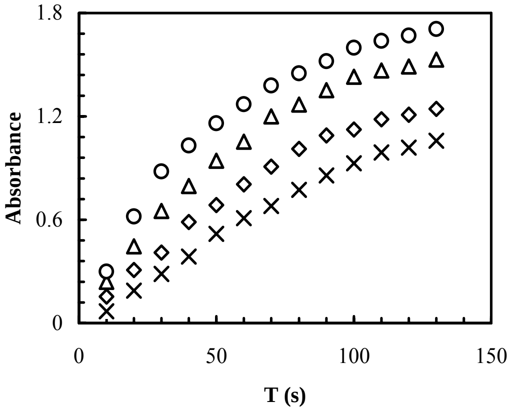

Fig. 2. Absorbance-time dependence plots of the dye formation reaction between substituted anilines and 4-AAP in presence of Rnp catalyst in water. (o) DMA, (Δ) *o*-toluidine, (◊) *o*-Cl-Ani, (×) *m*-Cl-Ani, [Amine] = 1.79 × 10^{-3} M, [4-AAP] = 1.50 × 10^{-2} M, [Rnp] = 2.44 × 10^{-3} M.

dye depends on substituents present in the aniline derivatives and the values are given in Table 1. The plots of absorbance versus time for the aniline derivatives at constant concentrations of 4-AAP and Rnp are shown in Fig. 2. The logX *vs*. time plots derived from the absorbance-time dependence measurements are presented in Fig. 3. The rate constant values of compositional variations of aniline derivatives, 4-AAP and Rnp are given in Table 1. The reactivity of dye formation depends on the electron releasing (+I) and withdrawing (-I) substituents present in the aniline derivatives as reflected by the following trend: DMA > *o*-toluidine > *o*-Cl-Ani > *m*-Cl-Ani.

Effect of Ionic Strength on the Reaction Rate

In order to study the charge of the intermediate species, KNO_3 is chosen as the inert electrolyte for salt effect. The stacked UV-Vis spectra of dye formation at constant composition of DMA, 4-AAP and Rnp in presence of KNO_3 (0.2 M) are shown in Fig. 4. At the time of addition of the

Table 1. The Pseudo First Order Rate Constant Values for the Dye Formation Between Substituted Anilines and 4-AAP Catalyzed by Rnp at 25 ºC in Aqueous Medium

Substrate No.	[Amine] M × 10^3	[4-AAP] M × 10^2	Rnp [M] × 10^3	DMA (555 nm)[a] k (s^{-1}) × 10^2 (±0.02)	*o*-Toluidine (535 nm)[a] k (s^{-1}) × 10^2 (±0.02)	*o*-Cl-Ani (546 nm)[a] k (s^{-1}) × 10^2 (±0.04)	*m*-Cl-Ani (534 nm)[a] k (s^{-1}) × 10^2 (±0.04)
1	1.00	1.50	2.44	2.93	2.61	1.84	1.45
2	1.79	1.50	2.44	3.56	3.05	2.33	1.94
3	1.79	1.00	2.44	3.32	2.75	2.10	1.58
4	1.79	1.50	3.52	5.81	4.96	2.83	2.31
5	1.79	1.50	1.85	2.66	2.13	1.36	1.01

[a]λ_{max} of the resulting dye.

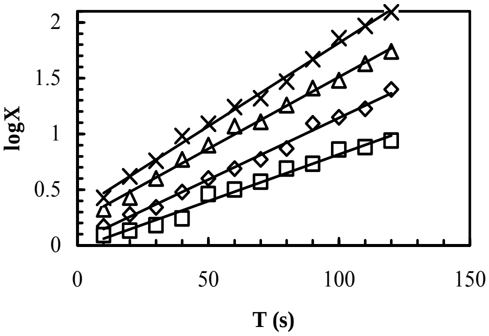

Fig. 3. The kinetic plots for the rate coefficient etermination for the dye formation reaction between substituted anilines and 4-AAP in presence of Rnp catalyst in water at 25 ºC. (o) DMA, (Δ) *o*-toluidine, (◊) *o*-Cl-Ani, (×) *m*-Cl-Ani, [Amine] = 1.79 × 10^{-3} M, [4-AAP] = 1.50 × 10^{-2} M, [Rnp] = 2.44 × 10^{-3} M.

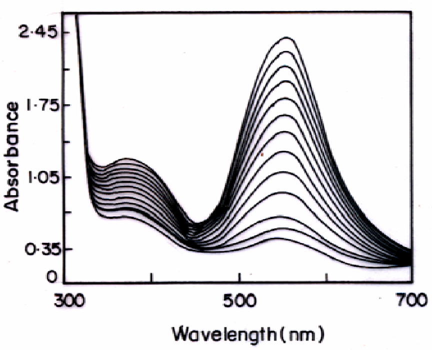

Fig. 4. UV-Vis stacked spectra at various time intervals for the dye formation reaction of AN with 4-AAP catalyzed by Rnp in aqueous medium at 25 ºC, in the presence of 0.2 M KNO_3. [DMA] = 1.79 × 10^{-3} M, [4-AAP] = 1.50 × 10^{-2} M, [Rnp] = 2.44 × 10^{-3} M.

Table 2. The Rate Constant Values of the Reaction between Aniline Derivatives and 4- AAP Catalyzed by Rnp at Different Concentrations of KNO_3 in Aqueous Media at 25 ºC. [Amine] = 1.79 × 10^{-3} M, [4-AAP] = 1.50 × 10^{-2} M, [Rnp] = 2.44 × 10^{-3} M

Substrate No.	$[KNO_3]$ M	DMA k^a	*o*-Toluidine k^a	*o*-Cl-Ani k^b	*m*-Cl-Ani k^b
1	0.1	0.47	0.37	0.28	0.23
2	0.2	0.64	0.53	0.35	0.27
3	0.3	0.97	0.66	0.44	0.34
4	0.4	1.36	1.01	0.66	0.46

$^a(s^{-1}) \times 10^1$ (±0.02). $^b(s^{-1}) \times 10^1$ (±0.04).

concentrations of KNO_3 (0.1 M, 0.2 M, 0.3 M and 0.4 M) are given in Table 2. It is found that the addition of KNO_3 generally increases the overall rate constant of the reaction.

Figure 6, generally referred to as a Bjerrum-Bjerrum plot, shows the log(rate) constant *vs*. $\sqrt{\mu}$, reflecting the effect of the ionic strength on the reaction between the aniline derivatives and 4-AAP as catalyzed by the Rnp system. For all the substrates, the slope value falls nearly to 1.0, indicating that the product of Z_AZ_B is nearly 1.0. Since the slopes are positive, the charge of the intermediate is considered to be +1. The positive charge of the intermediate explains the necessity for the acidic pH in the dye formation reactions. The reactivity trend observed among the anilines in the presence of Rnp (regardless of the KNO_3 concentration) is: DMA > *o*-toluidine > *o*-Cl-Ani > *m*-Cl-Ani.

Effect of pH on the Reaction Rate

The pH of the reaction was also found to have a significant role in the dye formation reaction [18,19]. We employed acetate and citrate-phosphate buffers ranging from 2.4-5.4 and the rate constant values at various pH levels are given in Table 3. The pH profiles of log(rate) constant *vs*. pH are shown in Fig. 7. The rate constant values are found to increase steadily up to a pH of 3.6 after which the rate constant value decreases. However, the dye formation reaction does not proceed in the basic medium. In the acidic medium, anilines are protonated to anilinium ion in which the *para* position is activated [20]. Further reaction with 4-AAP at the *para* position leads to

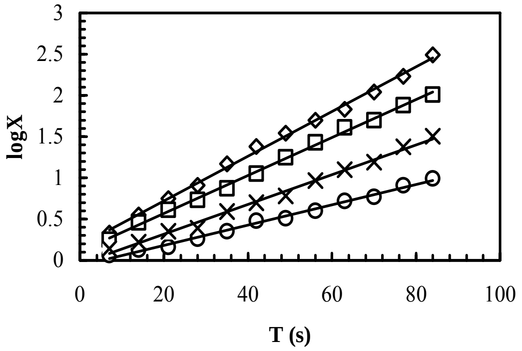

Fig. 5. The kinetic plots for the rate coefficient determination of substituted anilines with 4-AAP catalyzed by Rnp in aqueous medium at 25 ºC, in the presence of 0.2 M KNO_3. (◊) DMA, (□) *o*-toluidine, (×) *o*-Cl-Ani, (o) *m*-Cl-Ani, [Amine] = 1.79 × 10^{-3} M, [4-AAP] = 1.50 × 10^{-2} M, [Rnp] = 2.44 × 10^{-3} M.

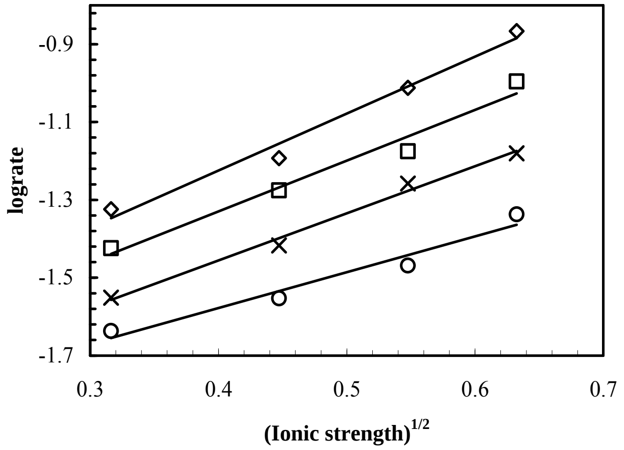

Fig. 6. Ionic strength effect on the rates of reaction between aniline derivatives and 4-AAP catalyzed by Rnp in the presence of KNO_3. (◊) DMA, (□) *o*-toluidine, (×) *o*-Cl-Ani, *m*-(o) Cl-Ani.

Table 3. Effect of pH on the Rate Constant Values of Rnp Catalyzed Dye Formation Reaction Between Substituted Anilines and 4-AAP in Aqueous Media at 25 ºC. [Amine] =1.79 × 10^{-3} M, [4-AAP] = 1.50 × 10^{-2} M, [Rnp] = 2.44 × 10^{-3} M

Substrate No.	pH	DMA K^a	*o*-Toluidine k^a	*o*-Cl-Ani k^b	*m*-Cl-Ani k^b
1	2.6	1.12	0.83	0.56	0.30
2	3.6	1.58	1.32	0.88	0.59
3	4.4	0.52	0.46	0.35	0.19
4	5.4	0.44	0.39	0.28	0.16

$^a(s^{-1}) \times 10^1$ (±0.02). $^b(s^{-1}) \times 10^1$ (±0.04).

the dye formation. At the optimum pH of 3.6, the trend of reactivity for the aniline substrates is as follows: DMA > *o*-toluidine > *o*-Cl-Ani > *m*-Cl-Ani.

Influence of Temperature on the Reaction Rate

The effect of temperature on the rate of dye formation was examined with temperatures ranging from 25 ºC to 65 ºC [21]. In all cases, the catalytic activity is enhanced as the temperature increases (Table 4). The rate constant value increases with an increase in temperature, reaching a maximum at 50 ºC. When the temperature increases to 65 ºC, the rate constant value decreases correspondingly, possibly maintained a low concentration of catalyst and substrate while studying the effect of temperature. Thus, the reaction temperature of 50 ºC is suggested for maximum rate constant values. The Arrhenius plots of the log of the rate constant *vs*. 1/T are shown in Fig. 8.

The linear plots with negative slope values are used to calculate the activation energy as shown in Table 4. The reactivity trend observed in anilines, based on the rate constant values, is DMA > *o*-toluidine > *o*-Cl-Ani > *m*-Cl-Ani.

Reaction Mechanism

The overall reaction is given in Scheme 1 and the reaction pathway, involving *m*-chloro aniline with 4-AAP to produce antipyrilquinoneimine dye using the catalyst Rnp, is presented in Scheme 2. In an acidic pH, the protonated form of the amine exists in equilibrium with the nonprotonated species

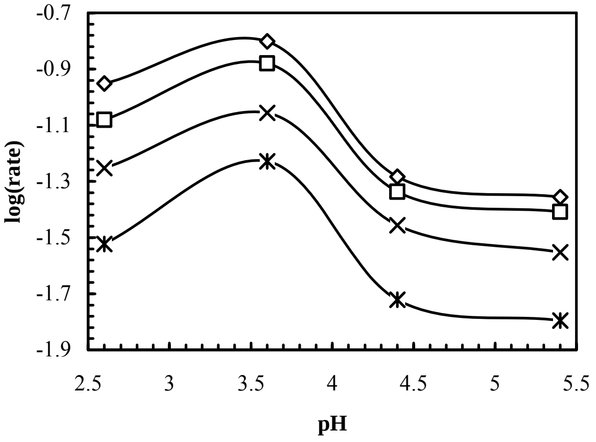

Fig. 7. pH profiles for the log of the reaction rates of the Rnp-catalyzed reaction between 4-AAP and various substituted anilines at 25 ºC in aqueous medium. (◊) DMA, (□) *o*- toluidine, (×) *o*-Cl-Ani, (o) *m*-Cl-Ani.

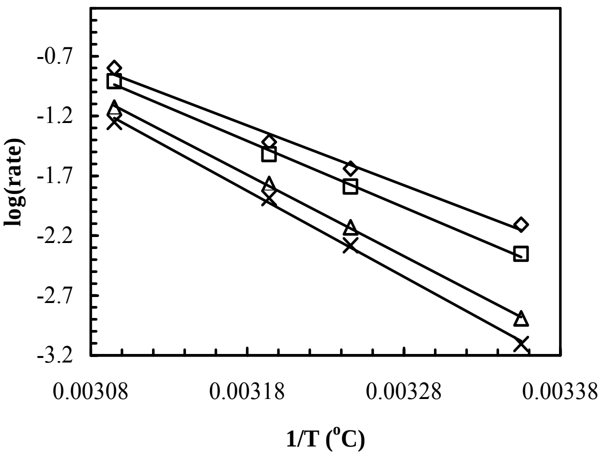

Fig. 8. Arrhenius plots for the reaction of various aniline substrates with 4-AAP catalyzed by Rnp in aqueous medium. (◊) DMA, (□) *o*-toluidine, (Δ) *o*-Cl-Ani, (×) *m*-Cl-Ani.

Table 4. Arrhenius Activation Parameter and the Rate Constant Values of the Dye Formation Reaction of Anilines with 4-AAP Catalyzed by Rnp at Various Temperatures. [Rnp] = 3.16 × 10^{-4} M, [Amine] = 2.31 × 10^{-4} M, [4-AAP] = 2.70 × 10^{-3} M

Substrate No.	Substrates	E_a (kcal mol^{-1}) (±0.05)	25 °C k_1 (s^{-1}) × 10^3 (±0.03)	35 °C k_2 (s^{-1}) × 10^2 (±0.03)	40 °C k_3 (s^{-1}) × 10^2 (±0.03)	50 °C k_4 (s^{-1}) × 10^2 (±0.04)	65 °C k_5 (s^{-1}) × 10^2 (±0.04)
1	N,N-Dimethyl aniline	19.70	7.77	2.29	3.83	10.2	6.87
2	*o*-Toluidine	23.68	4.42	1.62	3.02	9.84	6.54
3	*o*-Chloro aniline	32.00	1.28	0.74	1.71	8.43	4.05
4	*m*-Chloro aniline	34.73	0.78	0.53	1.30	7.36	3.27

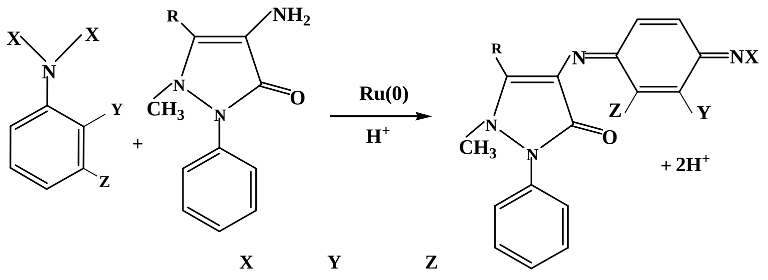

		X	Y	Z
DMA	:	**$(CH_3)_2$**	**H**	**H**
o-Toluidine	:	**H**	**CH_3**	**H**
o-Chloro aniline	:	**H**	**Cl**	**H**
m-Chloro aniline	:	**H**	**H**	**Cl**

Scheme 1

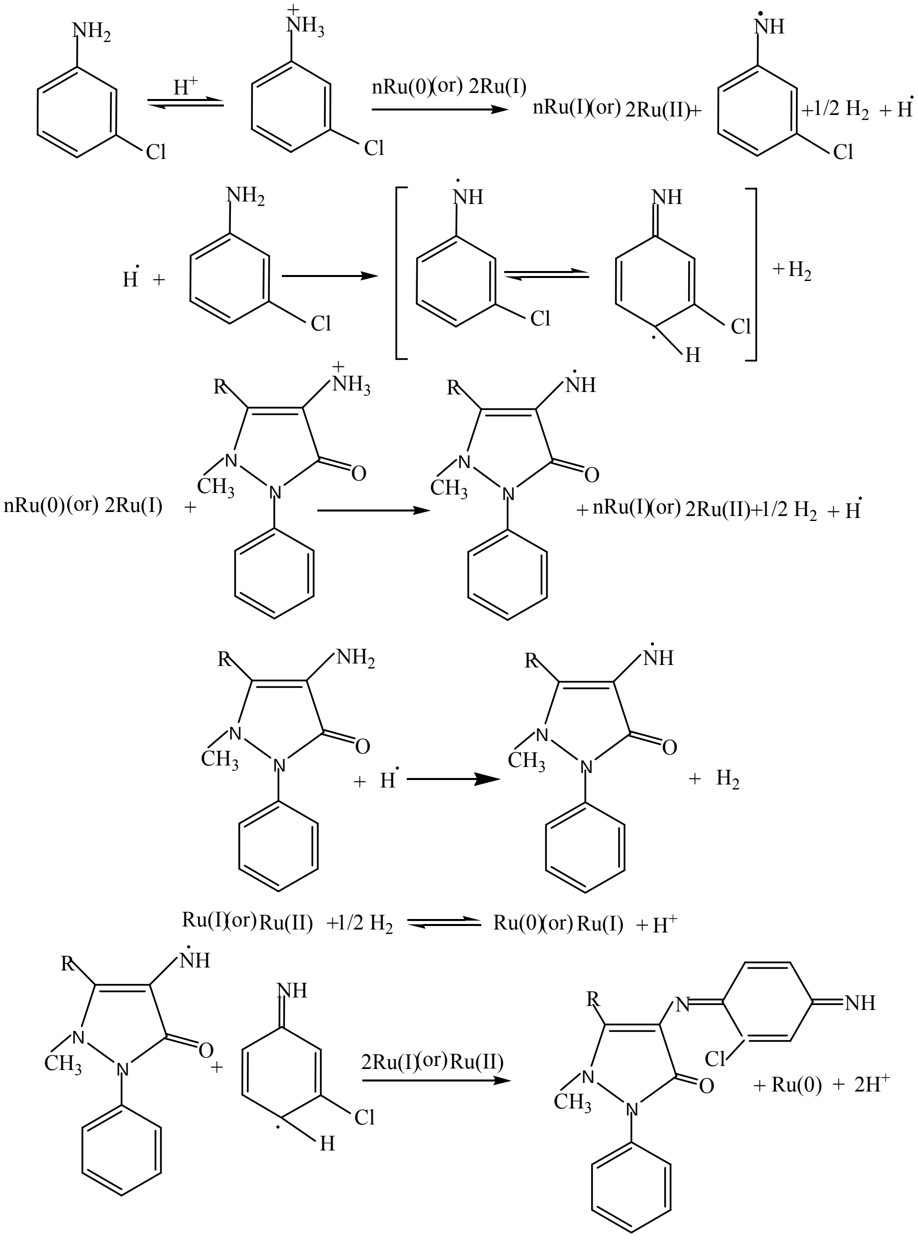

Scheme 2

[22]. When Rnp is added to this reaction mixture, $H^{\bullet}$ radical-tagged 4-AAP and *m*-Cl aniline are associated with the generation of Ru(I) or Ru(II). The main reactive species $H^{\bullet}$ is generated during the conversion of Ru(0) to Ru(I) or Ru(II). The unstable and highly reactive species $H^{\bullet}$ generated from deprotonated aniline derivatives produces the imino radical.

The resultant radical can undergo a coupling reaction with the 4-aminoantipyril radical in the presence of Ru(I) or Ru(II). Subsequently, the recombination of these two radical species produces a colored antipyrilquinoneimine dye. In order to confirm the presence of radicals during the reaction course, a few drops of acrylonitrile are added, after which a white polymer product is observed which subsequently precipitates out of the medium after some time. The concomitant radical

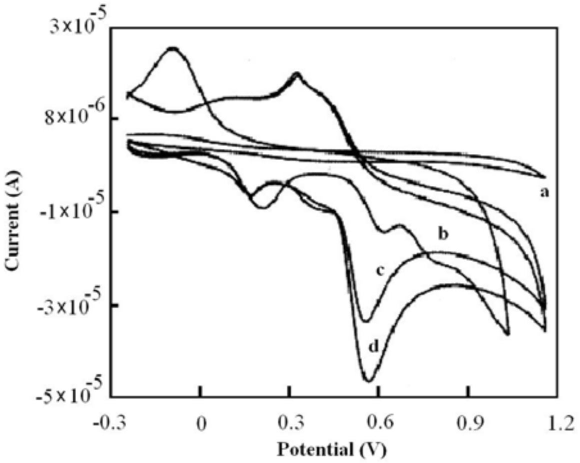

Fig. 9. Cyclic voltammograms of the dye formed from the reaction between DMA and 4-AAP in the presence of Rnp with the supporting electrolyte H_2SO_4 (0.5 M) and Pt and Ag/AgCl as working and reference electrodes, respectively, at 25 ºC. (a) Rnp, (b) Rnp + reactant at 30 s, (c) Rnp + reactant at 3 min and (d) Rnp + reactant at 8 min.

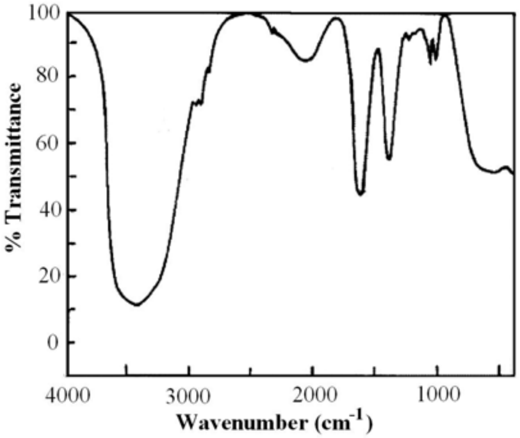

Fig. 10. FT-IR spectra of the Rnp dye containing DMA system taken in KBr pellet at 25 ºC.

activation of amine with 4-AAP along with the activation by Ru(0) are the contributing factors for the rate enhancement in the presence of nanoparticles.

The dye product, characterized using the FT-IR spectra for the DMA system shown in Fig. 9, gave a peak at 1635 cm^{-1} corresponding to [-C_B = N-], where C_B refers to the benzene ring carbon of the amine and N is from an amino group of 4-AAP.

The cyclic voltammograms of the dye formed from DMA in the presence of the Rnp catalyst are given in Fig. 10. Here, platinum and Ag/AgCl wires were used as the working and reference electrodes, respectively. In aqueous solution, a 0.43 V peak is observed for the Rnp catalyst, and upon the addition of substrates, a new peak is observed at 0.587 V in the anodic region due to the binding of Rnp with DMA and 4-AAP. Figure 11 shows a TEM photograph of Rnp synthesized by adopting a polyol method using PVP as a capping agent. A particle size of 7 nm is confirmed for the Rnp.

CONCLUSIONS

The studied dye formation reaction between substituted anilines and 4-AAP catalyzed by Rnp revealed pseudo first order kinetics with respect to each reactant. Regarding the study of the variables of substrates, pH, salt and temperature, the reaction does not proceed in the absence of the catalyst nor at basic pH. The observed rate constants for anilines with electron donating groups are greater than those with electron withdrawing groups. In the presence of salt the rate constant values steadily increase along with increasing KNO_3 concentrations. At acidic pH values, the rate constant of the reaction increases to a maximum rate at pH 3.6. The activation energy of aniline derivatives with electron donating groups is lower than those with electron withdrawing groups. Based on the rate constant values, the reactivity trend among the aniline systems is: DMA > *o*-toluidine > *o*-Cl-Ani > *m*-Cl-Ani. This observed reactivity trend remains the same regardless of the levels of the different variables tested. The report illustrates a novel spectrophotometric technique for the detection of aromatic amines in aqueous solutions *via* coupling reaction.

REFERENCES

[1] L.S. Debruin, J.B. Pawliszyn, P.D. Josephy, Chem. Res. Toxicol. 12 (1999) 78.

[2] S. Mishra, V. Singh, A. Jain, K.K. Verma, Analyst 126 (2001) 1663.

[3] E.A. Clark, R. Anliker, O. Hutzinger, The Handbook of Environmental Chemistry Berlin: Springer-Verlag 3A

(1980) 181.

[4] D.A. Villalobos, I.D. Buchanan, J. Environ. Eng. Sci. 1 (2002) 65.

[5] M. Oyama, K. Kirihara, Electrochimica. Acta 49 (2004) 3801.

[6] M. Kadar, Z. Nagy, T. Karancsi, G. Farsang, Electrochimica. Acta 46 (2001) 1297.

[7] E. Pramauro, A.B. Prevot, V. Augugliaro, L. Palmisano, Analyst 120 (1995) 237.

[8] E.H. Seymour, N.S. Lawrence, E.L. Beckett, J. Davis, R.G. Compton, Talanta 57 (2002) 233.

[9] E. Brillas, E. Mur, R. Sauleda, L. Sanchez, J. Peral, X. Domenech, J. Casado, Appl. Catal. B: Environ. 16 (1998) 31.

[10] N. Rajendiran, J. Santhanalakshmi, J. Mol. Catal. A: Chem. 245 (2006) 185.

[11] C. Degrand, B. Limoges, A.-M. Martre, B. Schollhorn, Analyst 126 (2001) 887.

[12] W.W. Yu, H. Liu, J. Mol. Catal. A: Chem. 243 (2006) 120.

[13] M. Cerro-Alarcon, A. Maroto-Valiente, I. Rodrıguez-Ramos, A. Guerrero-Ruiz, Carbon 43 (2005) 2711.

[14] A. Spitaleri, P. Pertici, N. Scalera, G. Vitulli, M. Hoang, T.W. Turney, M. Gleria, Inorganica. Chimica. Acta 352 (2003) 61.

[15] A. Roucoux, J. Schulz, H. Patin, Chem. Rev. 102 (2002) 3757.

[16] X. Yan, H. Liu, K.Y. Liew, J. Mater. Chem. 11 (2001) 3387.

[17] F. Bonet, V. Delmas, S. Grugeon, R. Herrera Urbina, P.-Y. Silvert, T.-K. Elhsissen, Nano Str Materials 11 (1999) 1277.

[18] K. Tamaoku, Y. Murao, K. Akiura, Y. Ohkura, Anal. Chem. Acta 136 (1982) 121.

[19] W. Sun, H. Jiang, K. Jiao, J. Chem. Sci. 117 (2005) 317.

[20] S. Premsingh, N.S. Venkataramanan, S. Rajagopal, S.P. Mirza, M. Vairamani, S. Rao, K. Velavan, Inorg. Chem. 43 (2004) 5744.

[21] O.S. Feria, S. Duron, Int. J. Hydrogen Energy 27 (2002) 451.

[22] A.M. Grana, J.M. H-Ramon, R.A. Mosquera, Chem. Phys. Lett 412 (2005) 106.